

1 **Complex dissolved organic matter on the roof of the world – Tibetan DOM**
2 **molecular characteristics indicate sources, land use effects, and processing along**
3 **the fluvial-limnic continuum**

4

5 Philipp Maurischat ^{1,2}, Michael Seidel ³, Thorsten Dittmar ^{3,4}, Georg Guggenberger ¹

6 ¹ Institute of Soil Science, Leibniz University Hannover, 30419 Hannover, Germany

7 ² Institute of Biology and Environmental Sciences (IBU), Carl von Ossietzky University of Oldenburg,
8 26129 Oldenburg, Germany

9 ³ Institute for Chemistry and Biology of the Marine Environment (ICBM), Carl von Ossietzky University
10 of Oldenburg, 26129 Oldenburg, Germany

11 ⁴ Helmholtz Institute for Functional Marine Biodiversity at the University of Oldenburg (HIFMB), 26129
12 Oldenburg, Germany

13 **Correspondence to: Philipp Maurischat (philipp.maurischat@uni-oldenburg.de)**

14 **Keywords:** Non-metric multidimensional scaling (NMDS), Alpine pastures, Natural organic matter
15 (NOM), Land use controls, Molecular NOM composition, Fourier-transform ion cyclotron resonance
16 mass spectrometry (FT-ICR-MS)

17

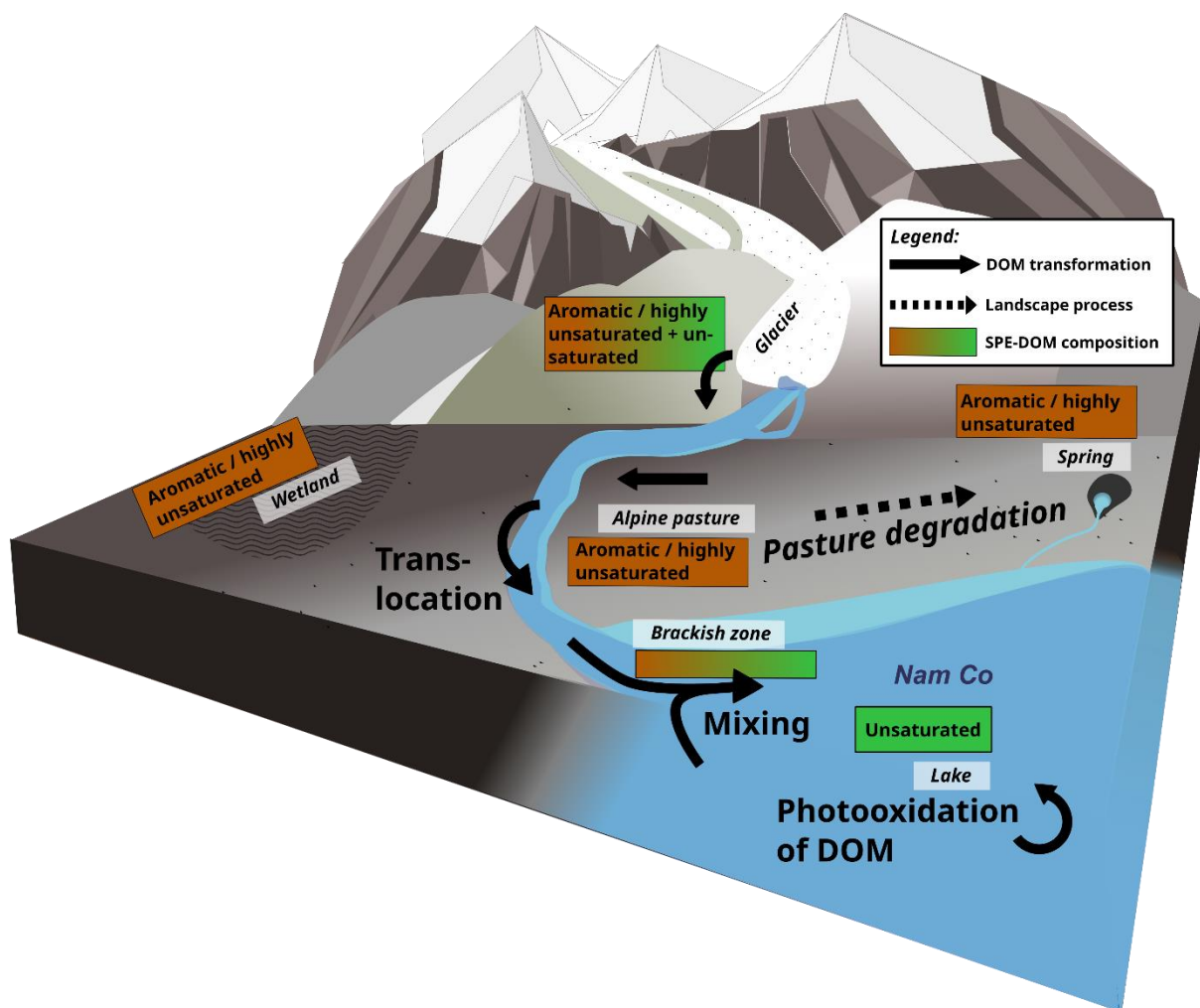
18 **Funding:** This research is a contribution to the International Research Training Group "Geo-ecosystems
19 in transition on the Tibetan Plateau (TransTiP)", funded by Deutsche Forschungsgemeinschaft (DFG
20 grant 317513741 / GRK 2309). Funding for MS by Cluster of Excellence EXC 2077 "The Ocean Floor –
21 Earth's Uncharted Interface" (Project number 390741603).

22

23 **Conflict of interest:** No conflict of interest.

24 Abstract

25 The Tibetan Plateau (TP) is the world's largest and highest plateau, comprising the earth's biggest
26 alpine pasture system. It is sensitive to impacts of climate change and anthropogenic pressure. Carbon
27 cycling on the TP is influenced by glaciation and degradation of the pasture ecosystem. Dissolved
28 organic matter (DOM) connects carbon reservoirs, following the hydrological continuum from glaciers
29 and headwaters to lakes. Due to its complexity, DOM cycling along the aquatic continuum and the
30 impact of land use and climate change on DOM characteristics are still not well understood. Here, we
31 study solid phase extracted (SPE) DOM molecular characteristics using ultrahigh-resolution mass
32 spectrometry (FT-ICR-MS) along the TP hydrological continuum from glaciers, groundwater springs,
33 and wetlands including pastures and alpine steppes, to the endorheic Lake Nam Co. Our study revealed
34 that the SPE-DOM composition was largely influenced by local sources of glaciers, wetlands, and
35 groundwater springs as well as pasture degradation. Glacial meltwater SPE-DOM contained more
36 saturated compounds suggesting microbial sources together with aromatic compounds probably
37 derived from aeolian deposition. In comparison, wetland and stream SPE-DOM were characterised by
38 a higher percentage of highly unsaturated and aromatic molecular formulae. These were likely derived
39 from inputs of vascular plants and soils. Groundwater spring SPE-DOM from degraded pastures
40 differed from intact pasture samples. In degraded systems a strongly oxidised signature with lowest
41 counts of P heteroatoms, lower O/C ratio and higher aromaticity of SPE-DOM together with a high
42 degradation index suggested a strong transformation of SPE-DOM. SPE-DOM of the endorheic lake was
43 richer in unsaturated molecular formulae compared to the tributaries. This suggest algae and microbial
44 sources and production in the lake. The SPE-DOM rich in aromatic and highly unsaturated formulae
45 visible in the brackish zone of the lake shore contrasted sharply with that of the lake samples. Aromatic
46 molecular formulae were strongly depleted in the lake deep water suggesting photooxidation of
47 riverine SPE-DOM. This indicates that alpine SPE-DOM signatures are shaped by small-scale catchment
48 properties, land degradation, and the influence of glaciers and wetlands. The close link of alpine SPE-
49 DOM composition to landscape properties is indicative for a strong susceptibility of DOM
50 characteristics to climatic and land use changes in High Asia.



51 **Graphical Abstract: Main processes shaping SPE-DOM molecular characteristics and transformations**
 52 **in the high-alpine Nam Co catchment. DOM processing and sources are indicated by black arrows.**
 53 **Pasture degradation is indicated by a dashed arrow.**

54

55 **1. Introduction**

56 Nutrient and energy cycles of ecosystems are connected by dissolved organic matter (DOM) fluxes
 57 (Spencer et al., 2014). DOM can connect fluvial ecosystems over hundreds of kilometres (Seidel et al.,
 58 2015) and links terrestrial and aquatic ecosystems (Goodman et al., 2011). Biogeochemical processing
 59 and DOM sources are known to shape the molecular composition of DOM (Liu et al., 2020; Roebuck et
 60 al., 2020; Seifert et al., 2016; Wilson and Xenopoulos, 2009). But how But how the DOM characteristics
 61 in alpine aquatic systems are influenced by different ecosystems and how DOM responds to ecosystem
 62 degradation is not well understood yet.

63 The Tibetan Plateau (TP) comprises the largest alpine pasture system in the world (Miehe et al., 2019)
 64 and is known as Asia's water tower (Bandyopadhyay, 2013), forming the source of large river systems.
 65 Large amounts of the water are stored in the ice masses of the TP, forming the largest frozen

66 freshwater reservoir outside the polar regions. This third pole environment is well investigated (Qiu,
67 2008; Yao et al., 2012), revealing that High Asia's ecosystems are threatened (Hopping et al., 2018) by
68 climate change (Yao et al., 2019) and by intensification of land use (Harris, 2010). Furthermore,
69 emerging freshwater quality issues give reason for concern (Qu et al., 2019).

70 The Nam Co catchment, located in the southern part of the TP, lies in the transition zone of the *K.*
71 *pygmaea* dominated alpine pasture ecosystem (Miehe et al., 2008) and the alpine steppe. The unique
72 positioning in this transition zone is expressed between the south, with a more humid glacial-
73 influenced high-mountain ecosystem contrasting the hilly northern margin of the catchment, with
74 more arid climate and vegetation dominated by alpine steppe, where clear signs of pasture
75 degradation are visible (Maurischat et al., 2022). This makes the Nam Co catchment a suitable natural
76 laboratory to test for effects on organic matter (OM) characteristics and the cycling of OM in different
77 ecosystems (Anslan et al., 2020). The effects of pasture degradation of Tibetan soils on OM stocks have
78 been studied previously (Liu et al., 2017), but investigations on degradation induced changes of DOM
79 composition have fallen short. Also DOM characteristics and transformation in this complex natural
80 interplay have only been investigated to limited extent. Spencer et al. (2014) found complex OM
81 sources in glaciers, streams, and Lake Nam Co. A recent study highlighted a coupled decrease of
82 "protein-like" DOM with an increase of "humic-like" DOM along the flowpath (Li et al., 2021), whereas
83 other works found indications for less reactive stream DOM due to the cold and fast flowing water
84 (Maurischat et al., 2022). This leaves important questions of 1) how DOM signatures are influenced by
85 the diverse biotic and abiotic processes in the catchment with differing degrees of glaciation, alpine
86 wetlands, and groundwater sources, as well as land degradation, and the alpine pasture alpine steppe
87 ecotone, and 2) how DOM is processed along the streams and in the lake.

88 Fourier-transform ion cyclotron resonance mass spectrometry (FT-ICR-MS) is an ultrahigh-resolution
89 method allowing the identification of thousands of molecular formulae, offering an opportunity to
90 better understand molecular, solid phase extracted (SPE) DOM characteristics, sources, and
91 transformations (Hawkes et al., 2020; Leyva et al., 2020; Šantl-Temkiv et al., 2013). Here we used FT-
92 ICR-MS to decipher characteristics and processing of stream SPE-DOM of different subcatchments,
93 glaciers, a groundwater spring, an alpine wetland as well as SPE-DOM of an endorheic lake on the TP.

94 Our investigations aim at a better understanding of SPE-DOM processing at present conditions which
95 will help to assess the potential consequences of changing environmental conditions in the future. It
96 is important to link the potential vulnerability and responses of sensitive high-alpine ecosystems to
97 ongoing anthropogenic changes. In this respect, we hypothesized:

98 I) SPE-DOM derived from different ecosystems (glaciers, groundwater springs and wetlands) and
99 streams in degraded land possess unique DOM signatures compared to the integrated DOM of
100 subcatchment streams.

101 II) The SPE-DOM transformation along the stream path is limited, no major compositional shift is
102 expected in-stream.

103 III) The SPE-DOM characteristics of lake water are chemically distinct from the terrestrial DOM sources
104 and integrated stream SPE-DOM composition.

105 2. Materials and methods

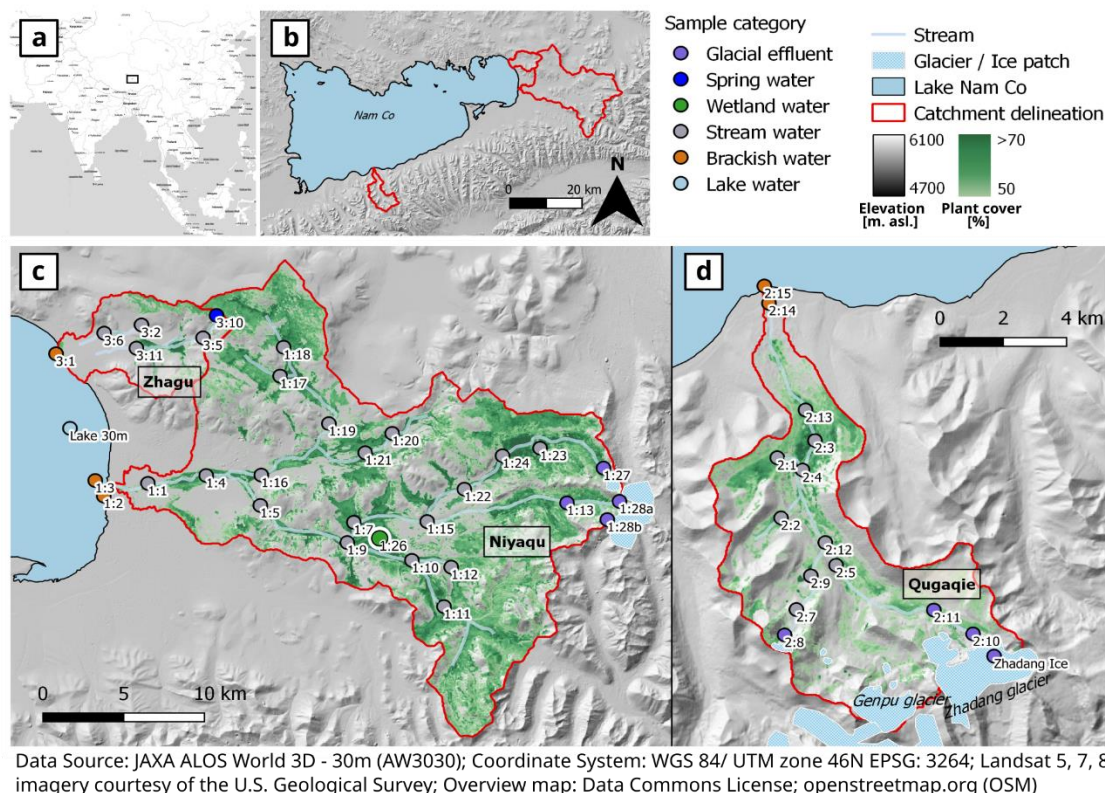
106 2.1 Site description and sampling

107 The Nam Co catchment has a total size of ~10800 km². Two main landscape units are distinguished, the
108 southern mountainous and the northern upland zone. The south of the catchment is characterised by
109 the Nyainqentanglha mountain ridge (NMR) with glaciation at highest elevations of more than 7000 m
110 asl. (Bolch et al., 2010). Glacial meltwater is the dominant water source of southern streams (Adnan
111 et al., 2019b). *K. pygmaea* pastures developed from 5300 m asl. downward (Anslan et al., 2020) and
112 are associated with a felty organic-rich topsoil (Kaiser et al., 2008). Closer to the lake alpine steppe
113 vegetation is prevailing (Nieberding et al., 2021). The southern part of the catchment is characterised
114 by higher precipitation compared to the north. Up to 530 mm y⁻¹ are measured at the NMR (Anslan et
115 al., 2020). In the hilly uplands a less steep relief dominates (Yu et al., 2021), and an annual precipitation
116 of around 300 mm y⁻¹ is reported (Anslan et al., 2020). Alpine pasture is developed in north-exposed
117 hill-flanks and valley bottoms, while alpine steppe grows on south exposed flanks, in the upland and
118 at the lake shoreline (Maurischat et al., 2022). Along with this aridity gradient from south to north,
119 land degradation is increasing (Anslan et al., 2020). The endorheic Lake Nam Co with an elevation of
120 4726 m asl. has a total size of ~2000 km². The lake is dimictic, oligotrophic, and lightly saline (0.9 g salt
121 l⁻¹; Keil et al., 2010) and has a depth of 99 m. It is well supplied with oxygen and has a clear water
122 column (Wang et al., 2020).

123 Three subcatchments of the Nam Co catchment were selected to represent the natural diversity (Fig.
124 1 a, b). The Niyaqu catchment (sample IDs 1:n in Fig. 1a, *low glaciation*) in the east has a total area of
125 406 km². Two streams drain the subcatchment, the southern stream receives meltwater from a glacier
126 of the NMR located 700 m above lake level. This river runs through extensive alpine pastures and feeds
127 a large alpine wetland (Fig. 1b, point 1:26). The northern stream drains a hilly upland area in the
128 transition of the alpine steppe and the alpine pasture. The herding of yaks takes place throughout the
129 year. The Zhagu subcatchment (sample IDs 3:n Fig. 1a, *no glaciation - degraded*) is located in the arid
130 north. It has a size of 46 km² and is mainly characterised by hilly upland relief (Keil et al., 2010). There

131 is no glacial influence and only a small altitudinal gradient in this catchment, with the highest elevation
 132 at 5230 m. asl. Two creeks drain the catchment, both fed by groundwater springs. During sampling,
 133 the streams were arheic, and clear signs of degradation of *K. pygmaea* pastures were visible
 134 (Maurischat et al., 2022). Besides degraded pastures, alpine steppe is developed and used for animal
 135 husbandry. In the south, the Qugaqie subcatchment (sample IDs 2:n Fig. 1b, *high glaciation*) represents
 136 the NMR zone. The catchment has a size of 58 km² and is characterised by steep relief and a valley
 137 course in south-north direction (Keil et al., 2010). The altitudinal difference between the lake and the
 138 summit is 2200 m. This catchment is used as summer pasture.

139 Water samples were taken in September 2019 following the streams from source to terminus. Glaciers,
 140 wetlands, and groundwater springs were sampled directly. Three source groups (glacial effluents,
 141 groundwater springs, and alpine wetlands) and three sampling units (stream water, brackish water,
 142 and lake water) were distinguished, resulting in six sample categories (Fig. 1). Glacial effluents were
 143 drawn directly at or close to the glacial terminus, while groundwater was sampled directly at springs.
 144 Alpine wetland samples were taken from the standing water column in the wetlands. Brackish water
 145 samples were taken in the mixing zone of stream and lake water offshore in Lake Nam Co.



146
 147 **Figure 1: (a) Overview map (Stamen Design, under CC BY 3.0. Data by Open Street Map contributors**
 148 **2022, under CC BY SA, distributed under the Open Data Commons Open Database Licence, ODbL,**
 149 **v1.0). The rectangle represents the sampling area. (b) Shows the outline of the Nam Co Lake and the**
 150 **three subcatchments. (c) and (d) Map of the investigated subcatchments and sampling locations**

151 **with sample categories. Plant cover estimations from Maurischat et al. (2022) represent *K. pygmaea***
152 **pastures, the zones of most prominent yak grazing.**

153 Samples were taken from the middle of the stream profile using a telescopic sampling device. Lake
154 water was sampled from 30 m depth with a submersible sampler. All samples were taken in seven
155 subsamples with a volume of 1 L each, mixed and a 0.5 L aliquot of this was taken for analysis. Samples
156 were filtered on-site using a 0.45 μm mesh size polyethersulfone membrane (Supor, Pall, Port
157 Washington, USA), a filtration device and a portable electric pump. Samples were stored in pre-cleaned
158 high-density polyethylene bottles (Rotilabo, Carl Roth, Karlsruhe, Germany) and kept at -21°C until
159 analysis.

160 2.2 Solid-phase extraction

161 DOM samples were acidified to pH 2 using 32 % HCl (Rotipuran p.a., Carl Roth, Karlsruhe, Germany).
162 Dissolved organic carbon (DOC) concentrations were measured from 20 mL of sample by high-
163 temperature oxidation on a total organic carbon analyser (varioTOC Cube, Elementar, Langenselbold,
164 Germany). DOM samples were diluted with ultrapure water to a concentration of 1.5 mg C L^{-1} , 250 mL
165 of diluted sample were used for extraction. Cartridges with 100 mg of styrene divinylbenzene polymer
166 (PPL) resin (Bond Elut, Agilent Technologies, Santa Clara, USA) were used for extraction. SPE-DOM was
167 prepared following Dittmar et al. (2008). The SPE elute was transferred to cauterized brown glass flasks
168 (Neochrom, Neolab Migge, Heidelberg, Germany) sealed with polytetrafluorethylen caps (Neochrom,
169 Neolab Migge, Heidelberg, Germany) and stored at -18°C until analysis. The extraction efficiency was
170 evaluated by drying 0.2 mL of SPE-DOM under N_2 atmosphere and resolving the aliquot in ultrapure
171 water. The samples were then analysed for their DOC concentrations by high temperature oxidation
172 and the volumetric proportion of initial DOC to extracted SPE-DOC concentrations was calculated.
173 Reference material (Suwannee River / IHSS) (Green et al., 2015) was compared with routine assays.
174 Blank samples with ultrapure water were used to check for contamination.

175 2.3 Fourier-Transform Ion Cyclotron Resonance Mass Spectrometry

176 SPE-DOM samples were diluted in 1:1 methanol/ultrapure water to a final concentration of 5 mg C L^{-1}
177 for analysis. Samples were analysed in duplicates on a Solarix XR 15 Tesla FT-ICR-MS (Bruker Daltonik,
178 Bremen, Germany). Electrospray ionization (ESI) was carried out in negative mode and samples were
179 injected at a flow rate of $122 \mu\text{L h}^{-1}$. 200 broadband scans (mass range of 92.14 to 2000 Da) were
180 acquired per sample, accumulation time was 0.2 s per scan. Mass spectra were internally calibrated
181 with a list of known $\text{C}_x\text{H}_y\text{O}_z$ molecular formulae over the mass range in the samples, achieving a mass
182 error of $< 0.1 \text{ ppm}$. Instrument variability was assessed with an in-house standard of SPE-DOM from
183 North Equatorial Pacific Intermediate Water (NEqPIW) collected near Hawaii (Natural Energy

184 Laboratory of Hawaii Authority, NELHA) (Green et al., 2014). Molecular formula attribution was done
185 with ICBM-OCEAN (Merder et al., 2020). The method detection limit (MDL) was applied (Riedel and
186 Dittmar, 2014) with a minimum signal-to-noise ratio (S/MDL) of 2.5. Minimum signal to MDL ratio as
187 backbone for recalibration was 5 using mean recalibration mode. Molecular formulae were assigned
188 with a tolerance of 0.5 ppm as $C_{1-100}H_{1-125}O_{1-40}N_{0-4}S_{0-2}P_{0-1}$ in the mass range 95 to 1000 Da. Molecular
189 formulae assignments were accepted if the molecular formula was present in >5% of the samples.
190 Contaminants were identified and excluded using the contaminant reference mass list and in
191 additional conformity with the SPE-DOM process blanks. Detection limits for peaks were normalised
192 to sample peak intensities. The overall peak intensities were scaled to the local sample maxima using
193 the sum of peaks. Molecular formulae containing isotopes (^{13}C , ^{18}O , ^{15}N , ^{34}S) were removed from the
194 data table for further processing and molecular formulae with molar ratios of oxygen-to-carbon (O:C)
195 = 0, O:C \geq 1, and hydrogen-to-carbon (H:C) > 2.5 were removed as well. Duplicate samples were
196 normalised, and molecular formulae were retained only when present in both duplicates.

197 2.4 SPE-DOM molecular descriptive classes, counts, and indices

198 Molecular formulae were assigned to SPE-DOM molecular compound classes (Leyva et al., 2020). The
199 original compound classification was taken from Šanti-Temkiv et al. (2013), and SPE-DOM compound
200 class labels were modified according to Merder et al. (2020). The modified aromaticity index (AI_{mod})
201 representing SPE-DOM aromaticity, was calculated for each formula as proposed by Koch and Dittmar
202 (2006; 2016). $AI_{mod} > 0.5$ was assigned as aromatic, while $AI_{mod} \geq 0.67$ was considered as condensed
203 aromatic compounds. The degradation index (I_{Deg}) was calculated as a measure of degradation state of
204 SPE-DOM (Flerus et al., 2012) and the terrestrial index (I_{Terr}) was calculated, as a measure of terrestrial
205 SPE-DOM sources (Medeiros et al., 2016). Molecular formulae that were part of the island of stability
206 (IOS) were evaluated to gain insight into the relative abundance of recalcitrant SPE-DOM (Lechtenfeld
207 et al., 2014). This is based on the assumption that the IOS contains SPE-DOM molecular formulae
208 representing recalcitrant oceanic SPE-DOM that is empirically stable on millennial time scales
209 (Lechtenfeld et al., 2014). The CHO index was calculated as a measure of organic carbon oxidation
210 (Mann et al., 2015). Low CHO values indicate highly reduced molecular formulae and high CHO values
211 indicate highly oxidised molecular formulae. Molecular diversity was interpreted as α -diversity by
212 depicting intracommunity molecular diversity (Thukral, 2017). Here we used the total number of
213 molecular formulae on the group scale of subcatchments and sample categories.

214 2.5 Statistical analyses

215 Molecular formula intensities were rescaled between 0 and 1. Grouping was conducted with two
216 independent factors: 1) the three subcatchments: Niyaqu (*low glaciation*), Qugaqie (*high glaciation*),
217 Zhagu (*degraded*) and Lake Nam Co; and 2) the sample categories: glacial effluents, spring, and wetland

218 as well as stream water, brackish water, and lake water. Samples from spring and wetland, as well as
219 Lake Nam Co, were excluded from statistical group comparisons due to the small sample sizes.
220 Intensity weighted arithmetic means, and standard deviations were calculated for AI_{mod} , number of
221 formulae containing the heteroatoms nitrogen (N), phosphorous (P) and sulphur (S), as well as the
222 total number of assigned formulae and for compound classes.

223 Due to violations of normal distribution and homoscedasticity in combination with unbalanced
224 sampling design, parametrical tests were considered unreliable (Bortz and Schuster, 2010). Multiple
225 pairwise comparisons were conducted using Kruskal-Wallis tests in combination with Bonferroni post
226 hoc corrected Dunn tests (Birnbaum, 1956). Significance levels of $\alpha = 0.05$ were applied
227 (Supplementary material, Table S1 and Table S2).

228 Nonmetric multidimensional scaling (NMDS) was used for dimensionality reduction and ordination
229 (Anderson et al., 2006; Faith et al., 1987) based on a Bray-Curtis dissimilarity index matrix ($k = 3$). Data
230 for NMDS were scaled and mean-centred (Jolliffe, 2002). NMDS was performed for independent
231 factors (sites and sample categories), while those with low statistical power ($n < 3$) were not
232 incorporated. Loadings, scores, and R^2 -coefficients of determination are provided in the
233 supplementary material (Tables S3 – S7). Co-correlation was checked visually and by Pearson's
234 correlation coefficient, defined as $|r| > 0.75$. The following compound classes were combined because
235 of co-correlation: aromatic O-rich and aromatic O-poor = ARO, highly unsaturated O-rich and highly
236 unsaturated O-poor = HUSAT, unsaturated O-rich, unsaturated O-poor and unsaturated with N = USAT
237 (Fig. 4). Collinear variables (section 2.6) were removed.

238 R software (The R project for statistical computing, v3.6.3, GNU free software) was used for statistics.
239 The R base packages (R Core Team, 2013) and *tidyverse* (Wickham et al., 2019) were used for data
240 organisation, pre-processing, and statistics. The packages *ggplot2* (Wickham et al., 2019) and *vegan*
241 (Oksanen et al., 2020) were used for graphical illustration and for NMDS analysis, respectively.

242 2.6 Environmental variables for statistical analysis

243 Several parameters were used as predictor variables in the NMDS. Internal predictor variables were
244 generated from the SPE-DOM dataset obtained by FT-ICR-MS (SPE-DOM indices, compound class
245 percentages and heteroatom counts; described in section 2.4). External predictor variables were taken
246 from a previous study of the same site and the same sampling campaign (Maurischat et al. 2022) and
247 tested for statistical correlations with this SPE-DOM dataset. The selected external variables showed
248 evidence as functional predictors in the prior study and are acknowledged as key parameters for DOM
249 characterisation in numerous applications. The variables included fluorescent DOM (FDOM)
250 components (here used as the product of co-correlated microbial and terrestrial-like FDOM

251 components) (Fellman et al., 2010), DOC concentrations (Eklöf et al., 2021), $\delta^{13}\text{C}$ of DOC (Guo et al.,
252 2006), dissolved inorganic carbon (DIC) concentrations, as a catchment geology parameter (Wang et
253 al., 2016), nitrate concentrations (NO_3^-) (Harms et al., 2016), and the mean plant cover at the sampling
254 point as land use indicator (Sankar et al., 2020).

255 3. Results

256 3.1 Sample treatment and quality assessment

257 SPE-DOM extraction efficiencies were $61.4\% \pm 18.6\%$ (Supplementary material, Table S8). DOM
258 extraction efficiencies and the number of SPE-DOM molecular formulae (detected by FT-ICR-MS) were
259 only weakly correlated ($R^2=0.08$, $F(1, 43)=5.144$, $\beta=-0.007$, $p=0.02$) indicating that extraction efficiency
260 was not an important driver of molecular variability in our samples. Duplicate SPE-DOM process blanks
261 had below 1000 molecular formulae assigned and the Suwannee River / IHSS reference material had
262 ~ 3500 . Minimum molecular formulae count to accept NOM samples was set to 2000, roughly in the
263 range of the number of molecular formulae expected from terrestrial aquatic samples (Seidel et al.,
264 2017; Spencer et al., 2014). The in house-control standard (NEqPIW SPE-DOM) was run repeatedly
265 during analysis ($n = 38$) to account for instrument variability. On average, $3558 (\pm 218)$ molecular
266 formulae were assigned: no significant instrument drift was detected (Supplementary material Figure
267 S1).

268 3.2 Molecular group counts and statistics

269 The number of assigned molecular formulae, here termed α -diversity, decreased in the order Qugaqie
270 (*high glaciation*) > Zhagu (*degraded*) > Niyaqu (*low glaciation*) > Lake Nam Co. Lake Nam CO SPE-DOM
271 had 50 % less assigned molecular formulae compared to the subcatchments (Table 1). SPE-DOM
272 samples from wetland and brackish environments had the highest numbers of assigned molecular
273 formulae (Table 2), compositional shifts in the H/C and O/C ratio of brackish and lake SPE-DOM are
274 displayed in Figure 6a with a zoom on one example mass range (371-371.3 m/z , Fig. 6b).

275 Lake Nam Co SPE-DOM had relatively more N-containing molecular formulae compared to SPE-DOM
276 samples from the subcatchments (Table 2). The relative abundance of S-containing molecular formulae
277 was significantly lower in *low glaciation* Niyaqu compared to *high glaciation* Qugaqie SPE-DOM
278 ($p=0.005$). P-containing molecular formulae were enriched in the lake compared to SPE-DOM of the
279 subcatchments (Table 1, Table S1). N-containing molecular formulae were more abundant in wetland
280 water and brackish SPE-DOM samples, while groundwater spring SPE-DOM samples had the lowest
281 count. Glacial SPE-DOM had the highest relative abundances of S-containing molecular formulae.

282 SPE-DOM of Lake Nam Co had lower Al_{mod} and I_{Terr} values, compared to the subcatchments (Table 1).
283 For the sample categories, brackish SPE-DOM had higher I_{Terr} values but no significant differences were

284 observed (Table 2). The H/C ratios were highest in Lake SPE-DOM (Table 1) with significantly higher
285 relative numbers of hydrogen compared to Niyaqu ($p=0.005$). Additionally, the CHO index showed that
286 Lake SPE-DOM and SPE-DOM of the *high glaciated* Qugaqie catchment were less oxidized compared
287 to SPE-DOM of the *degraded* Zhagu catchment ($p=0.042$ | statistically tested only for subcatchments).
288 Correspondingly, I_{Deg} values, were significantly higher for *degraded* Zhagu compared to the *glaciated*
289 Niyaqu and Qugaqie subcatchments SPE-DOM ($p=0.0002$). IOS values, indicative of recalcitrant SPE-
290 DOM with relatively long residence times, showed a significantly higher contribution in *degraded*
291 Zhagu and Lake Nam Co compared to *low glaciated* Niyaqu and *high glaciated* Qugaqie ($p= 0.04, 0.05,$
292 respectively| statistically tested only for subcatchments). For sample categories (Table 2), H/C ratios
293 were higher in glacial and lake SPE-DOM and the CHO index suggested less oxidized SPE-DOM in glacial
294 effluents and the lake compared to terrestrial sources (Fig. 5). Correspondingly highest I_{Deg} values were
295 observed in SPE-DOM of the brackish zone and in groundwater springs. The percentage of IOS values
296 increased in lake and groundwater springs compared to glacial effluents, indicating differences in the
297 contribution of recalcitrant SPE-DOM.

298 Compound classes (Fig. 2) give an overview of the composition of SPE-DOM. Largest differences among
299 the sites were found for aromatic classes. Lake Nam Co had 80 % less aromatic (O)-rich molecular
300 classes compared to the subcatchments. The lake had only 5 % of the abundance of aromatic O-poor
301 compounds compared to subcatchment SPE-DOM. For highly unsaturated O-rich molecular formulae,
302 Lake Nam Co had higher values compared to subcatchment SPE-DOM, while highly unsaturated O-
303 poor molecular formulae decreased in the lake. Furthermore, the unsaturated O-poor and unsaturated
304 N-containing SPE-DOM classes were higher in lake SPE-DOM compared to the terrestrial systems.
305 Highly unsaturated O-rich formulae were more abundant in SPE-DOM of *high glaciation* Qugaqie
306 compared to *low glaciation* Niyaqu (Fig. 2).

307 **Table 1: Overview on mean and standard deviation of indices and elemental composition ratios and**
 308 **mean and standard deviation of molecular formulae counts for sites.**

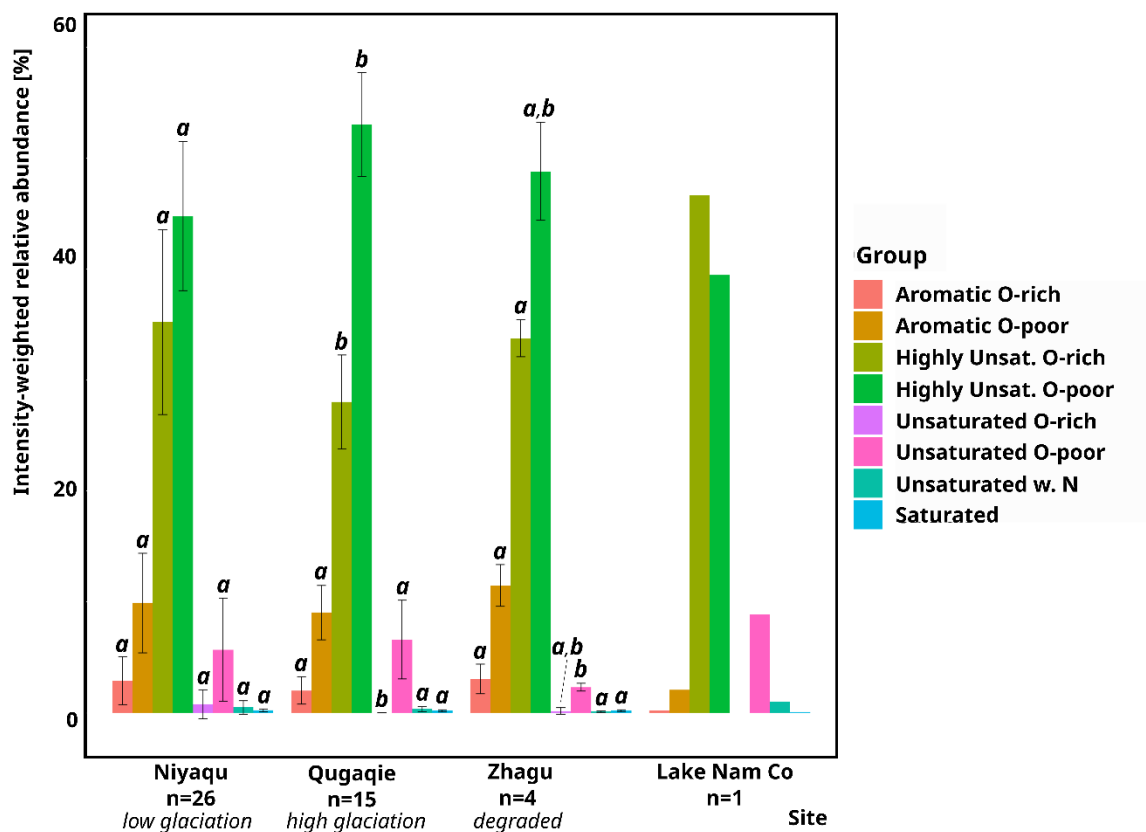
Variable	Niyaqu (<i>low glaciation</i>) n=26		Qugaqie (<i>high glaciation</i>) n=15		Zhagu (<i>degraded</i>) n=4		Lake Nam Co † n=1	
	Mean	SD (±)	Mean	SD (±)	Mean	SD (±)	Value	
AI _{mod}	0.33 ^a	0.05	0.32 ^a	0.02	0.36 ^a	0.02	0.25	
O/C	0.46 ^a	0.02	0.45 ^a	0.02	0.45 ^a	0.02	0.44	
H/C	1.12 ^a	0.08	1.17 ^b	0.05	1.13 ^{ab}	0.08	1.20	
CHO	-0.21 ^{ab}	0.11	-0.26 ^b	0.08	-0.17 ^a	0.04	-0.29	
I _{Deg}	0.55 ^a	0.15	0.59 ^a	0.10	0.77 ^b	0.02	0.33	
I _{Terr}	0.32 ^a	0.13	0.35 ^a	0.03	0.34 ^a	0.04	0.08	
IOS [%]	14.4 ^a	1.7	14.7 ^a	1.6	18.0 ^b	2.2	17.2	
Number of formulae containing N	1412 ^a (49.2)	941	1928 ^a (54.9)	1083	1933 ^a (56.5)	951	1284 (58.8)	
Number of formulae containing P	143 ^a (4.9)	112	129 ^a (3.6)	96	130 ^a (3.8)	54	196 (8.9)	
Number of formulae containing S	69 ^a (2.4)	96	146 ^b (4.1)	101	46 ^{ab} (1.3)	43	37 (1.6)	
Total number of molecular formulae (α-diversity)	2867 ^a	1060	3509 ^a	1340	3416 ^a	848	2183	

309 ^{a, b} Significant differences ($\alpha=0.05$) are indicated by superscript letters. † Single sample, standard
 310 deviations were not calculated and statistical tests were not performed. For heteroatoms (N, P, S),
 311 percentages of the total number of molecular formulae are given in parentheses. Boxplots of data are
 312 presented in the supplementary material (Fig. S2).

313 **Table 2: Overview on mean and standard deviation of indices and elemental composition ratios and**
 314 **mean and standard deviation of formulae counts for sample categories.**

Variable	Glacial effluent n=8		Spring † n=1	Wetland † n=1	Stream water n=38		Brackish water n=4		Lake water † n=1
	Mean	SD (±)	Value	Value	Mean	SD (±)	Mean	SD (±)	Value
AI _{mod}	0.31 ^a	0.04	0.35	0.33	0.33 ^a	0.05	0.35 ^a	0.02	0.25
O/C	0.45 ^a	0.03	0.44	0.46	0.46 ^a	0.02	0.46 ^a	0.01	0.44
H/C	1.17 ^a	0.08	1.15	1.09	1.13 ^a	0.07	1.13 ^a	0.07	1.20
CHO	-0.28 ^a	0.14	-0.18	-0.19	-0.22 ^a	0.09	-0.18 ^a	0.07	-0.29
I _{Deg}	0.53 ^a	0.13	0.77	0.53	0.58 ^a	0.15	0.66 ^a	0.02	0.33
I _{Terr}	0.34 ^a	0.06	0.32	0.34	0.32 ^a	0.11	0.39 ^a	0.04	0.08
IOS [%]	13.7 ^a	2.24	17.4	16.0	15.1 ^a	1.9	14.5 ^a	1.33	17.2
Number of formulae containing N	1548 ^a (52.2)	1135	1261 (44.7)	2549 (62.3)	1511 ^a (44.2)	922	2586 ^a (57.5)	1231	1284 (58.8)
Number of formulae containing P	103 ^a (3.4)	90	117 (4.1)	291 (7.1)	130 ^a (3.8)	91	231 ^a (5.1)	160	196 (8.9)
Number of formulae containing S	134 ^a (4.5)	125	9 (0.3)	68 (1.6)	77 ^a (2.2)	90	163 ^a (3.6)	126	37 (1.6)
Total number of formulae (α-diversity)	2965 ^a	1132	2819	4091	3416 ^a	1053	4492 ^a	1639	2183

315 ^{a, b} Significant differences ($\alpha=0.05$) are indicated by superscript letters. [‡] Single sample, standard deviations
 316 were not calculated and statistical tests were not performed. For heteroatoms (N, P, S), percentages of the
 317 total number of molecular formulae are given in parentheses. Boxplots of data are presented in the
 318 supplementary material (Fig. S3).



319

320 **Figure 2: Relative intensity-weighted averages of SPE-DOM compound classes for stream water of the**
 321 **three subcatchments and Lake Nam Co (sites). For sample sizes $n < 3$, no standard deviations are given.**
 322 **Error bars indicate standard deviations, significant differences ($\alpha=0.05$) are indicated by superscript**
 323 **letters (a, b).**

324 The relative abundances of aromatic compounds were different between SPE-Dom of the lake and SPE-
 325 DOM assigned to other sample categories, with samples from Nam Co having the lowest relative
 326 abundances (Fig. 3). Brackish SPE-DOM had significantly more aromatic O-poor compounds compared to
 327 glacial effluents ($p=0.05$). SPE-DOM from the Nam Co Lake had the highest relative abundances of highly
 328 unsaturated O-rich compounds compared to all other groups, especially glacial SPE-DOM had on average
 329 40% less O-rich compounds.

330 Unsaturated O-poor compounds were relatively more abundant in lake SPE-DOM and glacial effluents
 331 compared to the other environmental sample categories; this class was especially depleted in spring
 332 SPE-DOM. Alongside Lake and glacial SPE-DOM were relatively rich in unsaturated N-containing
 333 formulae. Spring water had the fewest of this compound class (Figure 3).

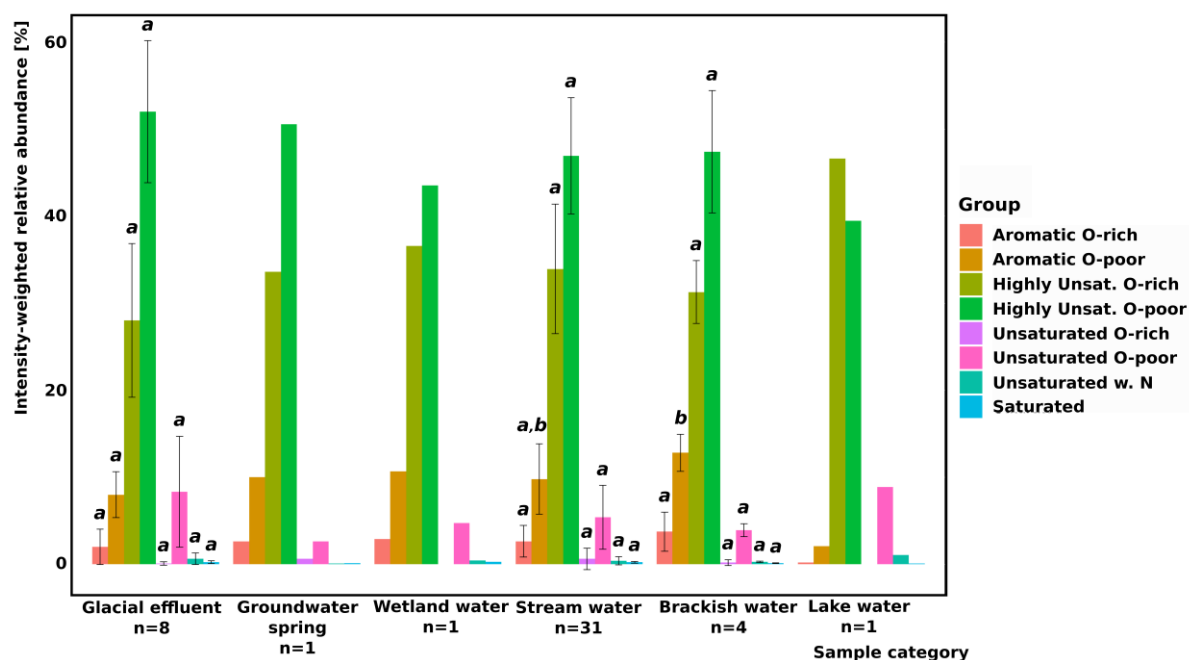


Figure 3: Relative intensity-weighted averages of DOM compound classes according to environmental sample categories. Error bars indicate standard deviations. For sample sizes $n < 3$, no standard deviations are given. Error bars indicate standard deviations, significant differences ($\alpha = 0.05$) are indicated by superscript letters (a, b).

334 3.3 Multivariate statistical analysis

335 NMDS was conducted with a graphical overlay for sites and sample categories. The stress value of 0.14
 336 is within tolerance (< 0.2 ; Dexter et al., 2018). In NMDS ordination (Fig. 4a) molecular formulae
 337 expanded in the ordination plane above the coordinate origin. Samples were distributed in two groups
 338 depending on aromaticity and related indicators (AI_{mod} , I_{Deg} , and I_{Terr}). AI_{mod} values increased from the
 339 positive to the negative direction of the first dimension. In the positive direction of dimension 1,
 340 samples containing relatively more unsaturated and saturated SPE-DOM compound classes as well as
 341 S-containing compounds were distributed (Fig. 4b) these samples also had lower AI_{mod} , I_{Deg} , and I_{Terr} . In
 342 the negative direction of dimension 1, samples with a higher abundance of aromatic compound classes
 343 were distributed. The external predictors DIC and plant cover were loading in this direction along with
 344 DOC concentrations and values of FDOM and $\delta^{13}C$ of DOM (black vectors in Fig. 4b) suggesting that
 345 these samples were influenced by DOM inputs of plants and soils. The second dimension of the NMDS
 346 ordination separated samples according to the abundance of highly unsaturated and saturated SPE-

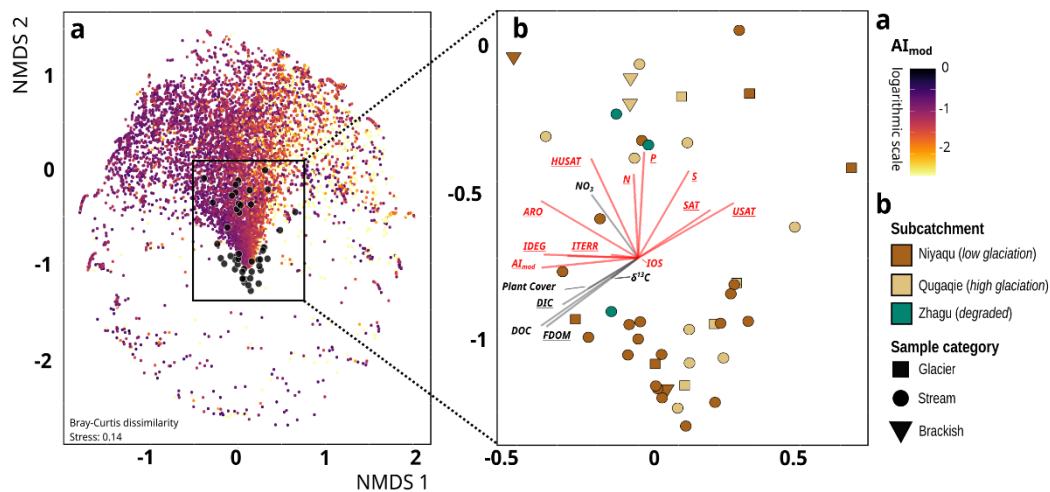
347 DOM compounds, together with the N, P and S heteroatoms. These samples were also characterized
348 by elevated NO₃ concentrations. Samples located closer to the origin of predictor variable vectors were
349 related to higher IOS percentages and suggested a higher abundance of recalcitrant SPE-DOM.

350 Samples of the *degraded* Zhagu subcatchment were located close to the centre of predictor variable
351 vectors (Fig. 4b), while samples of *high glaciation* Qugaqie were scattered on the dimension plane.
352 SPE-DOM from the *low glaciation* Niyaqu subcatchment as more uniformly placed in the lower part.
353 Stream water SPE-DOM was scattered, indicating large chemical diversity. Most brackish SPE-DOM
354 samples were placed in the upper left of the plane, associated with higher terrestrial indicators (AI_{mod},
355 I_{Deg}, and I_{Terr}) and more abundance of N and P heteroatoms. Glacial SPE-DOM was associated with
356 heteroatoms, saturated and unsaturated molecular compounds, and less depleted δ ¹³C of DOM,
357 visible by its positioning in the bottom left to top right of the ordination plane.

358 **4. Discussion**

359 **4. 1 Catchment properties shape SPE-DOM composition at Lake Nam Co**

360 The subcatchments (*high glaciation*, *low glaciation* and *degraded*) of Lake Nam Co differed significantly
361 in their molecular SPE-DOM composition. The *high glaciation* subcatchment had the largest molecular
362 α-diversity and a larger abundance of S heteroatoms (Table 1). This can be influenced by the
363 productivity of the glacial ecosystem (Hodson et al., 2008). S heteroatoms in DOM are likely related to
364 high sulphide contents in the runoff of Zhadang glacier (Yu et al., 2021). Sulphate reduction takes place
365 in glacial sediments and ice (Wu et al., 2012). Under sulfidic conditions, sulphide can be incorporated
366 into DOM (“sulfurization”) (Pohlabein et al., 2017). The higher abundance of O-poor compounds,
367 namely with depleted unsaturated O-rich and highly unsaturated O-rich molecular formulae and
368 increased highly unsaturated O-poor and unsaturated O-poor formulae alongside with negative CHO
369 values, indicates less intensively microbial transformed SPE-DOM compounds (Anesio et al., 2009;
370 Hood et al., 2009; Spencer et al., 2014) compared to the *degraded* and *low glaciation* subcatchments.
371 Accordingly, D’Andrilli et al. (2019) observed the relative increase of O-enriched molecular formulae
372 after bio-incubations of DOM. Likely, low water temperatures of the glacial meltwater in Qugaqie
373 hamper the microbial decomposition of DOM (Adams et al., 2010).



374

375 **Figure 4: Non-metric multidimensional (NMDS) scaling analysis based on the relative abundances of**
 376 **SPE-DOM molecular formulae (calculated on Bray–Curtis dissimilarity matrix) (a) with the colour-**
 377 **coded modified aromaticity index (AI_{mod} , logarithmic scale) (Koch and Dittmar 2006; 2016). b) Zoom**
 378 **of NMDS analysis based on the relative abundances of SPE-DOM molecular formulae with post-hoc**
 379 **fitted SPE-DOM parameters (internal predictor variables, red) and environmental parameters**
 380 **(external predictor variables, black) shown as vectors. Underlined parameters were significantly (p**
 381 **≤ 0.05) related to NMDS ordination (stress = 0.14, $k = 3$). ARO= aromatic O-rich and aromatic O-poor,**
 382 **HUSAT= highly unsaturated O-rich and highly unsaturated O-poor, USAT= unsaturated O-rich,**
 383 **unsaturated O-poor and unsaturated with N, and SAT= saturated. Subcatchments are represented**
 384 **by the colour of sample points, while sample categories are represented by shapes.**

385 Compared to the Qugaqie catchment, the contribution of glacial meltwater was smaller in the Niyaqu
 386 subcatchment and absent in Zhagu. The main water sources for Zhagu are precipitation and
 387 groundwater (Adnan et al., 2019a; Anslan et al., 2020; Tran et al., 2021). In the *degraded* Zhagu
 388 subcatchment, a stronger indication of aromaticity with higher AI_{mod} and higher relative abundance of
 389 aromatic compounds was found. Likewise, the higher oxidation state indicated by the CHO index (Fig.
 390 5b, Table 2) and higher degradation index (I_{Deg} , Table 2) suggest a larger share of soil-borne, aromatic
 391 DOM compounds This was also corroborated by the higher percentage of the IOS (+ ~3 %), indicating
 392 a larger input of degradation products. The *low glaciation* Niyaqu catchment in comparison had a
 393 higher contribution of aromatic and unsaturated compounds together with a lower H/C ratio,
 394 suggesting less oxidised DOM. In combination with the AI_{mod} and I_{Terr} indices this suggests inputs of soils
 395 and plants, with e.g. lignin and hemicellulose and their degradation products (Roebuck et al., 2018;
 396 Seifert et al., 2016).

397 The *high glaciation* Qugaqie catchment comprises of a signature rich in highly unsaturated O-poor and
 398 unsaturated O-poor formulae likely derived from a glacial-borne microbial source. Furthermore, the
 399 high aromatic indices (AI_{mod} , I_{Terr}) and high percentages of aromatic compound classes are indicative of
 400 SPE-DOM derived from soil and plant material. Likely, there is a steady input of soil-derived material
 401 into the streams from pastoral land as demonstrated for other grassland systems (Seifert et al., 2016;

402 Lu et al., 2015). Notably, this influence became smaller, when glacial-borne more unsaturated DOM
403 was more dominant on subcatchment level (Fig. 3b).

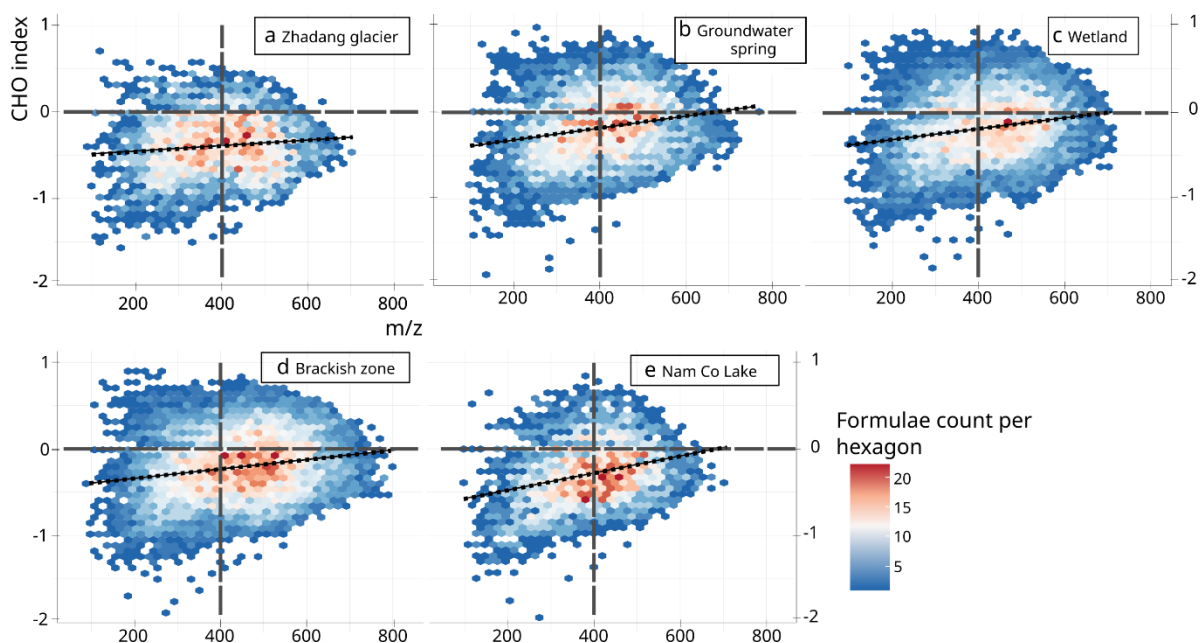
404 4.2 The effect of pasture degradation on SPE-DOM composition

405 Molecular α -diversity defined by the number of molecular formulae and SPE-DOM characteristics can
406 be pinpointed to landscape units / environmental sample categories (summarized in Fig. 7). Glacial
407 SPE-DOM from Qugaqie and Niyaqu subcatchments contained two different signatures from different
408 sources. First, with high abundances of unsaturated compounds with and without nitrogen as well as
409 a low oxidation state of carbon (Fig. 5a), high ratios of H/C and low percentages of recalcitrant SPE-
410 DOM visible by the IOS. These parameters indicate a relatively fresh, reduced (oxygen-poor) SPE-DOM
411 of low-molecular mass probably derived from microbial activity at the partly anoxic ice shield. This is
412 in-line with findings from other glacial environments worldwide (Hood et al., 2009; Telling et al., 2011;
413 Anesio et al., 2009). Second, aromatic and highly unsaturated compound classes and aromatic and
414 terrestrial indices (I_{Terr} , AI_{mod}) were suggesting plant- and soil-borne SPE-DOM sources, despite the
415 absence of plant cover in the glacial zones. Glaciers receive compounds with higher molecular mass
416 from aeolian deposition, either condensed (poly)aromatics, e.g. from the burning of fossil fuels
417 (Takeuchi, 2002) or compounds uncondensed but rich in phenolics, usually associated with dust from
418 degraded vascular plant material and soils (Singer et al., 2012). Local dust formation on the TP is
419 projected to increase with ongoing pasture degradation (Wang et al., 2008), likely affecting the DOM
420 composition of glaciers. The coexistence of microbial produced, autochthonous DOM and airborne
421 aromatic, allochthonous DOM renders the understanding of the downstream fate of glacial DOM
422 difficult.

423 Groundwater spring SPE-DOM from the *degraded* Zhagu subcatchment mainly contained aromatic and
424 highly unsaturated compounds. Molecular α -diversity and the number of N, P and S heteroatoms were
425 low. Together with this, high I_{Deg} and CHO indices suggested a strong degradation of spring SPE-DOM
426 (Fig. 5b) further 17% of DOM being IOS DOM indicates a large contribution of recalcitrant DOM. Spring
427 water is generally expected to inherit aquifer and catchment characteristics in its DOM signature, also
428 partly preserving its terrigenous source (Osterholz et al., 2022; Yoo et al., 2020). The shallow
429 groundwater table of Zhagu (Tran et al., 2021), is in contact with soil OM and yak faeces (Maurischat
430 et al., 2022), which can leach soil-borne OM to the groundwater (Connolly et al., 2020) which re-
431 emerge at groundwater springs. Hence, the highly degraded SPE-DOM compounds likely originated
432 from the degraded pedosphere and have been transported with the groundwater. The connection of
433 degraded pastures of Zhagu (Fig. 1 & 4b) with the molecular composition of groundwater spring SPE-
434 DOM indicates that highly modified SPE-DOM signatures are transported with the spring water and
435 retrieved in streams.

436 SPE-DOM of an alpine wetland had a high α -diversity (>4000 molecular formulae), was rich in N, and P
437 heteroatoms, as well as in highly unsaturated O-rich, and unsaturated O-poor compounds. The
438 wetland was also enriched in ammonium and DOC compared to the streams (Maurischat et al., 2022).
439 Alpine wetlands are highly productive and contain large amounts of nutrients in the biomass and soil
440 OM (Bai et al., 2010; Zhang et al., 2020). Wetlands on the TP have been massively degrading (Zhang et
441 al., 2011), enhancing microbial decomposition in wetland mire soils (Ma et al., 2018) and driving a
442 subsequent release of nutrients into adjacent streams (Gao, 2016). For Nam Co Lake this would pose
443 a severe biodiversity threat to oligotrophic streams and the sensitive lake shore (Hu et al., 2016).

444 Stream samples are concentrated in the lower centre of the NMDS (Fig. 4b). these samples had a
445 dominance of aromatic compounds either associated with highly unsaturated O-poor or highly
446 unsaturated O-rich formulae, suggesting mostly inputs of terrestrial compounds, such as lignin and
447 tannin and their degradation products (Mann et al., 2015), further corroborated by depleted $\delta^{13}\text{C}$ DOC
448 signatures (Fig. 4b; Maurischat et al., 2022). The *K. pygmaea* ecosystem spreads as an azonal pasture
449 along the streams (Fig. 1). Lu et al. (2015) pointed out that grassland sites provide terrestrial inputs of
450 aromatic and highly unsaturated compounds to surface waters. The *K. pygmaea* pasture browsed by
451 yak has potential influence of their faeces (Du et al., 2021), suggesting lower molecular mass and
452 negative CHO inputs due to the reductive conditions in the yak gastrointestinal tract and
453 decomposition of plant-borne material therein (Fahey et al., 1983). Stream samples can therefore also
454 be under influence of changing inputs from the pasture ecosystem. Faeces inputs and products of their
455 microbial utilisation are likely associated with increases of N-containing unsaturated formulae and
456 saturated formulae (Vega et al., 2020). Pastoral land-use and pasture degradation both had a
457 considerable impact on stream SPE-DOM composition. While intact pastures released a highly
458 unsaturated and aromatic signature related to the pasture soils and plants, streams close to degraded
459 pastures were characterised by highly oxidized aromatic signatures and low molecular α -diversity.



460

461 **Figure 5: Hexagon scatters plot the count of the chemical formula in the space of the CHO index**
 462 **(Mann et al., 2015) and m/z . The black dotted lines represent the linear model of the CHO index and**
 463 **m/z of the respective sample, and the grey dashed lines split the plot into quadrants for orientation.**
 464 **The regression and ledger lines are printed to guide the eyes only. a) Ice from a glacier in *high***
 465 ***glaciation* Qugaqie, b) groundwater spring from the upland of *degraded* Zhagu (3:10), c) water from**
 466 **the standing water column of a wetland (1:26), d) water from the brackish zone of Lake Nam Co and**
 467 **a tributary stream (2:15) and e) water sample from 30 m depth of Lake Nam Co. Axis scales are fixed.**

468 4.3 The Lake reactor: photooxidation changes the SPE-DOM molecular composition

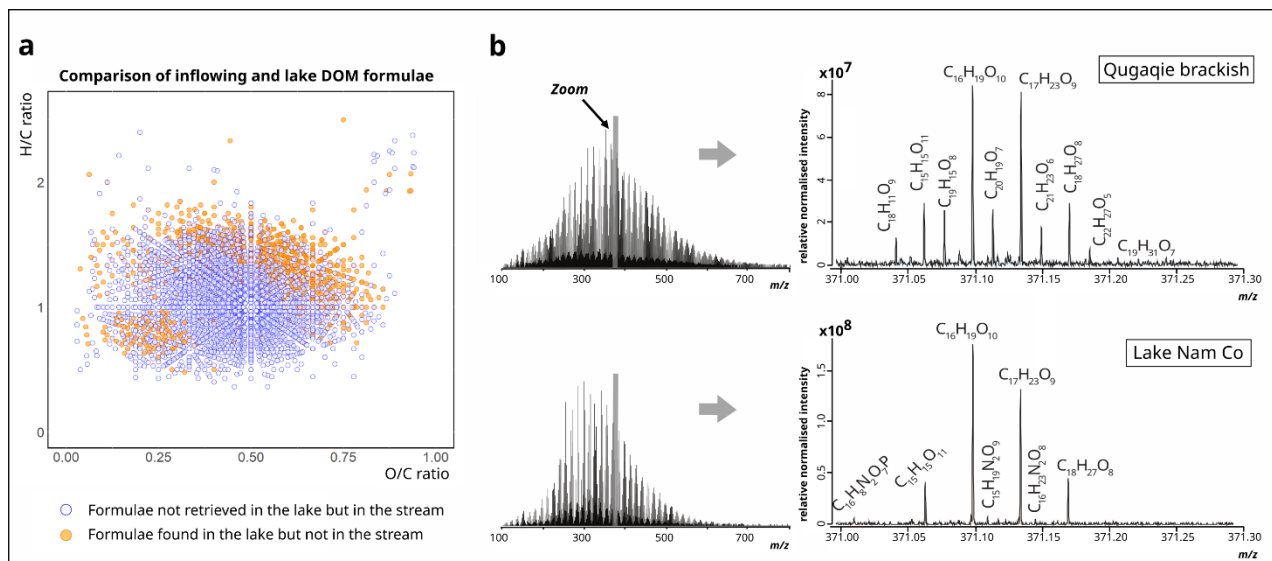
469 Brackish SPE-DOM samples had the highest molecular α -diversity, highest number of N and S
 470 heteroatoms and highest number of aromatic O-poor compounds together with high AI_{mod} and I_{Terr}
 471 (Tab. 2). Thus, brackish SPE-DOM retained and accumulated the terrestrial signal of streams. Brackish
 472 regions are not only zones of gradual mixing of different water masses (Van Dongen et al. 2008), where
 473 terrestrial-derived DOM of streams is exported to lakes and the ocean (Benner et al., 2004; Dittmar
 474 and Kattner, 2003; Ruediger, 2003) but are also zones of chemical transformation and uptake of
 475 riverine DOM, e.g. by flocculation and osmotrophy (Hoikkala et al. 2015). The relative increase of
 476 aromatic compounds in brackish SPE-DOM compared to stream SPE-DOM (Fig. 3) suggests a relative
 477 enrichment, for example, by selective degradation and oxidation of lower-molecular mass compounds
 478 in the wash of the waves as indicated by the increased CHO index and, I_{Deg} values (Fig. 5d) as shown
 479 for estuaries (Asmala et al., 2014). We conclude that the high molecular α -diversity in brackish samples
 480 represents both, the terrestrial input from streams mixing with the SPE-DOM signature of lake water
 481 and selective degradation of SPE-DOM in the high-energy wave zone.

482 Lake water differed in its SPE-DOM composition most strongly as compared to all other sample
 483 categories (Fig 7). Lake SPE-DOM was relatively enriched in unsaturated and saturated compounds,

484 which can include lipids and carbohydrates, but it was relatively depleted in aromatic and highly
485 unsaturated O-rich molecular formulae. Correspondingly, AI_{mod} and I_{Terr} decreased. Photooxidation and
486 microbial degradation can both remove aromatic DOM, such as lignin-derived phenolics (Spencer et
487 al. 2009; Helms et al. 2014; Vähätalo and Wetzel, 2004). Given the clear water column and high
488 irradiation at the TP (Wang et al., 2020), photooxidation can take place down to greater depths in the
489 lake, making it a probable important mechanism. Photooxidation in combination with microbial
490 degradation can explain the depletion of aromatic constituents when comparing brackish and lake SPE-
491 DOM (blue points in Fig. 6a and mass spectra in Fig. 6b).

492 In the estuary-lake gradient, riverine terrigenous SPE-DOM likely underwent a transformation, leaving
493 more recalcitrant SPE-DOM behind (Goldberg et al., 2015) as corroborated by the 2.1 % and 2.7 %
494 increase of IOS compared to stream and brackish SPE-DOM, respectively (Table 2). Along with
495 transformation of imported riverine SPE-DOM, primary production in the lake plays a key role for the
496 SPE-DOM characteristics of Lake Nam Co. The increase in unsaturated and unsaturated N-containing
497 compound classes and the more negative CHO with lower molecular mass (Fig. 5e) in lake SPE-DOM
498 (Fig. 3, yellow points in Fig. 6a) act as indicators for bacterial and algal primary production in the lake.
499 Microbial DOM sources have been suggested for Lake Nam Co (Spencer et al., 2014; Maurischat et al.,
500 2022) and other large lakes of the TP (Liu et al., 2020). Performing a food web study in Lake Nam Co,
501 Hu et al. (2016) reported that mainly lake-borne organic carbon sources are utilised by zooplankton,
502 showing the importance of this type of DOM as substrate. The comparably low CHO index (Fig. 5e)
503 underlines the existence of low molecular mass reduced DOM produced in the lake, while higher
504 molecular masses of aromatic and highly unsaturated riverine origin are more oxidised in the lake
505 environment compared to other systems (indicated by the greatest steepness of the regression line in
506 Fig. 5e), indicative of the strong processing described above. Lake SPE-DOM exhibited sources derived
507 from algal and microbial production. Also it is low in aromatic compounds and terrigenous indices and
508 had a much larger percentage of IOS as compared to subcatchment streams SPE-DOM, suggesting
509 more recalcitrant compounds. The shift in SPE-DOM molecular composition, hence, shows that the

510 terrigenous riverine aromatic DOM is processed in the lake, while microbiota derived DOM is
 511 produced.



512 **Figure 6: A) van Krevelen diagram of molecular formulae retrieved in lake DOM but not in brackish**
 513 **DOM and vice versa. B) Left: Intensity normalised overview mass spectra (m/z : 100-800) of Qugaqie**
 514 **brackish DOM (Id 2:15) and a water sample from 30 m depth of the Lake Nam Co. Right: Exemplary**
 515 **zoom into one mass range (371.0-371.3 m/z) of the respective samples. Note the axis scales shift.**

516

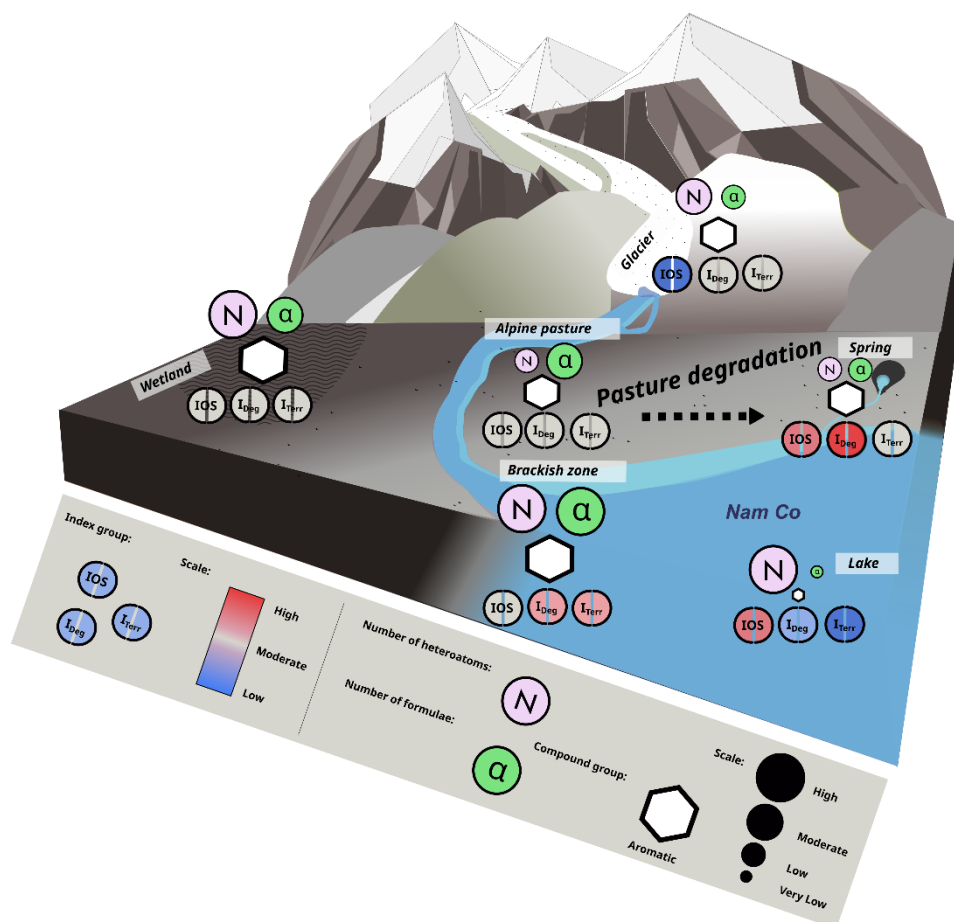
517 5. Conclusions

518 We elucidated the molecular composition and the processing of SPE-DOM in the High Asian endorheic
519 Nam Co catchment. We investigated three subcatchments: *high glaciation*, *low glaciation*, *no*
520 *glaciation / degraded*, including SPE-DOM samples of glaciers, groundwater springs, alpine wetlands,
521 streams, the brackish mixing zone, and the weakly saline lake. The subcatchments differed in the
522 molecular composition of SPE-DOM.

523 In the *high glaciation* catchment, we identified a unique dual source of a microbial, low-molecular
524 mass SPE-DOM relatively enriched in S heteroatoms and unsaturated compounds with and without
525 nitrogen, suggesting autotrophic sources in the glacial ice shield. Meanwhile, aromatic SPE-DOM with
526 high abundance of highly unsaturated compounds, such as plant-derived lignin degradation products
527 or polycondensed aromatics derived from the combustion of fossil fuels or household burning of yak
528 faeces, hint at a depositional source by aeolian transport. The influence of glacial meltwater greatly
529 modified SPE-DOM signatures along the *high glaciation* Qugaqie stream, probably delivering more bio-
530 available compounds to the southern lake shoreline. The *low glaciation* Niyaqu catchment comprised
531 a lower molecular α -diversity and had a mainly terrestrial-borne SPE-DOM source of highly
532 unsaturated and aromatic compounds, attributed to the input of the surrounding *K. pygmaea* pastures
533 to the streams. In comparison, spring SPE-DOM of the *degraded* Zhagu subcatchment was influenced
534 by degradation of *K. pygmaea* pastures visible by highly degraded and oxidized signatures with a higher
535 percentage of recalcitrant compounds. DOM signatures can thus be used to trace pasture degradation.
536 Wetland SPE-DOM exhibited high molecular α -diversity and was relatively enriched with N-
537 heteroatoms. Wetland SPE-DOM reflected the comparably high primary productivity of these systems.
538 The reported degradation of alpine wetlands in High Asia can drive a large release of DOM to the
539 streams; at Nam Co this can be considered a threat to the oligotrophic lake. The stream samples were
540 mostly associated with the input of terrestrial-borne materials, originating from vascular plants and
541 soils. These are attributed to the *K. pygmaea* ecosystem stretching along the paths of streams. From
542 the pastures, aromatic and highly unsaturated SPE-DOM was constantly refuelled into the streams.
543 Brackish SPE-DOM represented the mixing zone of stream and lake water. Here riverine terrestrial
544 DOM entered the lake, indicating that DOM transformation along the stream was limited. However,
545 lake SPE-DOM was different compared to the tributaries. Its molecular composition suggested
546 photooxidation and microbial degradation as transformation of imported stream DOM, together with
547 a source of microbial and algal production in the oligotrophic lake.

548 Our study shows that DOM cycling in the Nam Co catchment needs a thorough assessment, as it can
549 be diverse on subcatchment level and between landscape units. In order to safeguard water resources
550 and related ecosystem services, knowledge about the different sources and the fate of DOM is

551 indispensable. SPE-DOM molecular properties have proven to be selective for the source systems and
 552 hence allow to decipher landscape processes. In the case of the sensitive TP, they might be a way
 553 forward to better understand the local effects of global change.



554
 555 **Figure 7: Overview of the molecular information from SPE-DOM along the water continuum of the**
 556 **TP. The number of N-heteroatoms is indicated relative to the total number of molecular formulae.**
 557 **The island of stability (IOS), degradation index (I_{Deg}), and terrestrial index (I_{Terr}) are ranging in a red-**
 558 **blue colour. Alpine steppe and groundwater spring samples are spatially correlated, and thus subject**
 559 **of a common evaluation. The local pasture degradation gradient is indicated by a dashed arrow.**

560 Acknowledgements

561 The authors thank the staff of ITP-CAS and the NAMORS research station for their hospitality and
 562 assistance during the sampling campaign. We further thank the associated members of the TransTiP
 563 team for organizing the field work and helping hands during sampling.

564 This research is a contribution to the International Research Training Group "Geo-ecosystems in
 565 transition on the Tibetan Plateau (TransTiP)", funded by Deutsche Forschungsgemeinschaft (DFG grant
 566 317513741 / GRK 2309).

567
 568 M. Seidel is grateful for DFG funding within the Cluster of Excellence EXC 2077 "The Ocean Floor –
 569 Earth's Uncharted Interface" (Project number 390741603).

570 **References**

- 571 Adams H.E., Crump B.C., Kling G.W.: Temperature controls on aquatic bacterial production and
572 community dynamics in arctic lakes and streams. *Environmental microbiology*,12,5,1319–33,
573 2010.
- 574 Adnan M., Kang S., Zhang G., Saifullah M., Anjum M.N., Ali A.F.: Simulation and Analysis of the Water
575 Balance of the Nam Co Lake Using SWAT Model, *Water*, 11(7),2019a.
- 576 Adnan M., Kang S.C., Zhang G.S., Anjum M.N., Zaman M., Zhang Y.Q.: Evaluation of SWAT Model
577 performance on glaciated and non-glaciated subbasins of Nam Co Lake, Southern Tibetan
578 Plateau, China. *J. Mt. Sci.*, 16, 5, 2019b.
- 579 Anesio A.M., Hodson A.J., Fritz A., Psenner R., Sattler B.: High microbial activity on glaciers:
580 importance to the global carbon cycle. *Global Change Biol.*, 15, 4, 2009.
- 581 Anslan S., Azizi Rad M., Buckel J., Echeverria Galindo P., Kai J., Kang W. et al.: Reviews and syntheses:
582 How do abiotic and biotic processes respond to climatic variations in the Nam Co catchment
583 (Tibetan Plateau)? *Biogeosciences*, 17, 5, 1261–79, 2020.
- 584 Asmala E., Autio R., Kaartokallio H., Stedmon C.A., Thomas D.N.: Processing of humic-rich riverine
585 dissolved organic matter by estuarine bacteria: effects of predegradation and inorganic nutrients.
586 *Aquat Sci*, 76, 3, 451–63, 2014.
- 587 Bandyopadhyay, J.: Securing the Himalayas as the Water Tower of Asia: An Environmental
588 Perspective. *Asia Policy* 16, 2013.
- 589 Bai J., Ouyang H., Xiao R., Gao J., Gao H., Cui B. et al.: Spatial variability of soil carbon, nitrogen, and
590 phosphorus content and storage in an alpine wetland in the Qinghai - Tibet Plateau, China. *Soil*
591 *Res.*48, 8, 730, 2010.
- 592 Benner R., Benitez-Nelson B., Kaiser K., Amon R.M.W.: Export of young terrigenous dissolved organic
593 carbon from rivers to the Arctic Ocean. *Geophysical Research Letters*, 31, 5, 2014.
- 594 Birnbaum Z.W.: On a use of the Mann-Whitney Statistic. In: Neyman J., Editor. *Proceedings of the*
595 *Third Berkeley Symposium on Mathematical Statistics and Probability: Held at the Statistical*
596 *Laboratory, December 26-31, 1954. Berkeley, CA: University of California Press, 13–18, 1956.*
- 597 Bolch T., Yao T., Kang S., Buchroithner M.F., Scherer D., Maussion F. et al.: A glacier inventory for the
598 western Nyainqentanglha Range and the Nam Co Basin, Tibet, and glacier changes 1976–2009.
599 *The Cryosphere*, 4, 3, 2010.
- 600 Bortz J., Schuster C.: *Statistik für Human- und Sozialwissenschaftler: Limitierte Sonderausgabe. 7th ed.*
601 *Berlin, Heidelberg, Springer, 2010.*
- 602 Connolly C.T., Cardenas M.B., Burkart G.A., Spencer R.G.M., McClelland J.W.: Groundwater as a major
603 source of dissolved organic matter to Arctic coastal waters. *Nature communications*, 11, 1, 2020.
- 604 D’Andrilli J., Junker J.R., Smith H.J. et al.: DOM composition alters ecosystem function during
605 microbial processing of isolated sources. *Biogeochemistry*, 142, 281–298, 2019.
606 <https://doi.org/10.1007/s10533-018-00534-5>.
- 607 Dexter E., Rollwagen-Bollens G., Bollens S.M.: The trouble with stress: A flexible method for the
608 evaluation of nonmetric multidimensional scaling. *Limnol. Oceanogr. Methods*, 16, 7, 2018.

609 Dittmar T., Kattner G.: The biogeochemistry of the river and shelf ecosystem of the Arctic Ocean: a
610 review. *Marine Chemistry*, 83, 3-4, 2003.

611 Dittmar T., Koch B., Hertkorn N., Kattner G.: A simple and efficient method for the solid-phase
612 extraction of dissolved organic matter (SPE-DOM) from seawater. *Limnol. Oceanogr. Methods*, 6,
613 6, 2008.

614 Du Z., Wang X., Xiang J., Wu Y., Zhang B., Yan Y., et al.: Yak dung pat fragmentation affects its carbon
615 and nitrogen leaching in Northern Tibet, China. *Agriculture, Ecosystems & Environment*,
616 <https://www.sciencedirect.com/science/article/pii/S0167880921000050>, 2021.

617 Eklöf K., von Brömssen C., Amvrosiadi N., Fölster J., Wallin M.B., Bishop K.: Brownification on hold:
618 What traditional analyses miss in extended surface water records. *Water Res.*, Vol. 203, 117544,
619 2010. <https://doi.org/10.1016/j.watres.2021.117544>.

620 Fahey Jr. G.C., Jung H.G.: Lignin as a Marker in Digestion Studies: a Review. *Journal of Animal Science*,
621 Vol. 57, 1, 1983.

622 Fellman J.B., Hood E., Spencer R.G.M.: Fluorescence spectroscopy opens new windows into dissolved
623 organic matter dynamics in freshwater ecosystems: A review, *Limnol. and Oceanogr.*, 55, 2010.
624 DOI: 10.4319/lo.2010.55.6.2452

625 Flerus R., Lechtenfeld O.J., Koch B.P., McCallister S.L., Schmitt-Kopplin P., Benner R. et al.: A
626 molecular perspective on the ageing of marine dissolved organic matter. *Biogeosciences*, 9, 6,
627 1935–55, 2012.

628 Gao, J.: Wetland and Its Degradation in the Yellow River Source Zone. In: Brierley G., Li X., Cullum C.,
629 Gao J. (eds): *Landscape and Ecosystem Diversity, Dynamics and Management in the Yellow River*
630 *Source Zone*. Springer Geography. Springer, Cham. 2016.

631 Goldberg S.J., Ball G.I., Allen B.C., Schladow S.G., Simpson A.J., Masoom H., et al.: Refractory
632 dissolved organic nitrogen accumulation in high-elevation lakes. *Nat Commun*, 6, 6347, 2015.

633 Goodman K.J., Baker M.A., Wurtsbaugh W.A.: Lakes as buffers of stream dissolved organic matter
634 (DOM) variability: Temporal patterns of DOM characteristics in mountain stream-lake systems. *J.*
635 *Geophys. Res.*, 116, 1, 2011.

636 Green N.W., McInnis D., Hertkorn N., Maurice P.A., Perdue E.M.: Suwannee River Natural Organic
637 Matter: Isolation of the 2R101N Reference Sample by Reverse Osmosis. *Environmental*
638 *Engineering Science*, 32, 1, 2015.

639 Green N.W., Perdue E.M., Aiken G.R., Butler K.D., Chen H., Dittmar T. et al.: An intercomparison of
640 three methods for the large-scale isolation of oceanic dissolved organic matter. *Marine*
641 *Chemistry*, 161, 2014.

642 Guo L. and Macdonald, R.W.: Source and transport of terrigenous organic matter in the upper Yukon
643 River: Evidence from isotope ($\delta^{13}\text{C}$, $\Delta^{14}\text{C}$, and $\delta^{15}\text{N}$) composition of dissolved, colloidal, and
644 particulate phases, *Global Biogeochem. Cycles*, 20, GB2011, 2006.

645 Harms T. K., Edmonds J. W., Genet H., Creed I. F., Aldred D., Balsler A., Jones, J. B.: Catchment
646 influence on nitrate and dissolved organic matter in Alaskan streams across a latitudinal gradient,
647 *J. Geophys. Res. Biogeosci.*, 121, 350– 369, 2016.

648 Harris R.B.: Rangeland degradation on the Qinghai-Tibetan plateau: A review of the evidence of its
649 magnitude and causes, *Journal of Arid Environments*, 74, 1, 2010.

650 Hawkes J.A., D'Andrilli J., Agar J.N., Barrow M.P., Berg S.M., Catalán N. et al.: An international
651 laboratory comparison of dissolved organic matter composition by high resolution mass
652 spectrometry: Are we getting the same answer? *Limnol. Oceanogr. Methods*, 18, 6, 2020.

653 Helms J.R., Mao J., Stubbins A., Schmidt-Rohr K., Spencer R.G.M., Hernes P.J. et al.: Loss of optical
654 and molecular indicators of terrigenous dissolved organic matter during long-term
655 photobleaching. *Aquat Sci*, 76, 3, 2014.

656 Hodson A., Anesio A.M., Tranter M., Fountain A., Osborn M., Prisco J. et al.: GLACIAL ECOSYSTEMS.
657 Ecological Monographs, 78, 1, 41–67, 2008.

658 Hoikkala L., Kortelainen P., Soinne H., Kuosa H.: Dissolved organic matter in the Baltic Sea. *J. o.*
659 *Marine Systems*, Vol. 142, 2015.

660 Hood E., Fellman J., Spencer R.G.M., Hernes P.J., Edwards R., D'Amore D. et al.: Glaciers as a source
661 of ancient and labile organic matter to the marine environment. *Nature*, 462, 7276, 1044–7,
662 2009.

663 Hopping, KA, Knapp, AK, Dorji, T, Klein, JA.: Warming and land use change concurrently erode
664 ecosystem services in Tibet. *Glob Change Biol*. 24, 2018.

665 Hu E., He H., Su Y., Jeppesen E., Liu Z.: Use of Multi-Carbon Sources by Zooplankton in an Oligotrophic
666 Lake in the Tibetan Plateau. *Water*, 8, 12, 2016.

667 Jolliffe I.T.: Principal Component Analysis. New York, NY: Springer-Verlag New York Inc; 2002.

668 Keil A., Berking J., Mügler I., Schütt B., Schwalb A., Steeb P.: Hydrological and geomorphological basin
669 and catchment characteristics of Lake Nam Co, South-Central Tibet. *Quaternary International*,
670 218, 1-2, 2010.

671 Kaiser K., Miehe G., Barthelmes A., Ehrmann O., Scharf A., Schult M., Schlütz F., Adamczyk S., Frenzel
672 B.: Turf-bearing topsoils on the central Tibetan Plateau, China: Pedology, botany, geochronology.
673 *CATENA*, 73, 3, 300-311, 2008.

674 Koch B.P., Dittmar T.: From mass to structure: an aromaticity index for high-resolution mass data of
675 natural organic matter. *Rapid Commun. Mass Spectrom.*, 20, 5, 2006.

676 Koch B.P., Dittmar T.: From mass to structure: an aromaticity index for high-resolution mass data of
677 natural organic matter. *Rapid Commun. Mass Spectrom.*, 30, 1, 2016.

678 Lechtenfeld O.J., Kattner G., Flerus R., McCallister S.L., Schmitt-Kopplin P., Koch B.P.: Molecular
679 transformation and degradation of refractory dissolved organic matter in the Atlantic and
680 Southern Ocean. *Geochimica et Cosmochimica Acta*, 126, 2, 321–37, 2014.

681 Leyva D., Jaffe R., Fernandez-Lima F.: Structural Characterization of Dissolved Organic Matter at the
682 Chemical Formula Level Using TIMS-FT-ICR MS/MS. *Anal. Chem.*, 92, 17, 2020.

683 Li Y., Xiao K., Du J., Han B., Liu Q., Niu H. et al.: Spectroscopic fingerprints to track the fate of aquatic
684 organic matter along an alpine headstream on the Tibetan Plateau. *The Science of the total*
685 *environment*, 792, 148376, 2021.

686 Liu S., Schleuss P.-M., Kuzyakov Y.: Carbon and Nitrogen Losses from Soil Depend on Degradation of
687 Tibetan Kobresia Pastures. *Land Degrad. Develop.*, 28, 4, 1253–62, 2017.

688 Liu S., He Z., Tang Z., Liu L., Hou J., Li T. et al.: Linking the molecular composition of autochthonous
689 dissolved organic matter to source identification for freshwater lake ecosystems by combination

690 of optical spectroscopy and FT-ICR-MS analysis. *Science of The Total Environment*,
691 <https://www.sciencedirect.com/science/article/pii/S0048969719347552>, 2020.

692 Lu Y., Li X., Mesfioui R., Bauer J.E., Chambers R.M., Canuel E.A. et al.: Use of ESI-FTICR-MS to
693 Characterize Dissolved Organic Matter in Headwater Streams Draining Forest-Dominated and
694 Pasture-Dominated Watersheds. *PLOS ONE*, 10, 12, 2015.

695 Ma W., Alhassan A.R.M., Wang Y., Li G., Wang H., Zhao J.: Greenhouse gas emissions as influenced by
696 wetland vegetation degradation along a moisture gradient on the eastern Qinghai-Tibet Plateau
697 of North-West China. *Nutr. Cycl. Agroecosyst.*, 112, 2018.

698 Mann B.F., Chen H., Herndon E.M., Chu R.K., Tolic N., Portier E.F. et al.: Indexing Permafrost Soil
699 Organic Matter Degradation Using High-Resolution Mass Spectrometry. *PLOS ONE*, 10, 6, 2015.

700 Maurischat P., Lehnert L., Zerres V.H.D., Tran T.V., Kalbitz K., Rinnan Å. et al.: The glacial-terrestrial-
701 fluvial pathway: A multiparametrical analysis of spatiotemporal dissolved organic matter
702 variation in three catchments of Lake Nam Co, Tibetan Plateau. *The Science of the total
703 environment*, 156542, 2022.

704 Medeiros P.M., Seidel M., Niggemann J., Spencer R.G.M., Hernes P.J., Yager P.L. et al.: A novel
705 molecular approach for tracing terrigenous dissolved organic matter into the deep ocean. *Global
706 Biogeochem. Cycles*, 30, 5, 689–99, 2016.

707 Merder J., Freund J.A., Feudel U., Hansen C.T., Hawkes J.A., Jacob B. et al.: ICBM-OCEAN: Processing
708 Ultrahigh-Resolution Mass Spectrometry Data of Complex Molecular Mixtures. *Anal. Chem.* 92,
709 10, 2020.

710 Mieke G., Mieke S., Kaiser K., Jianquan L., Zhao X.: Status and Dynamics of the *Kobresia pygmaea*
711 Ecosystem on the Tibetan Plateau. *AMBIO: A Journal of the Human Environment*, 37, 4, 2008.

712 Mieke G., Schleuss P.-M., Seeber E., Babel W., Biermann T., Braendle M. et al.: The *Kobresia pygmaea*
713 ecosystem of the Tibetan highlands - Origin, functioning and degradation of the world's largest
714 pastoral alpine ecosystem: *Kobresia* pastures of Tibet. *The Science of the total environment*, 648,
715 754–71, 2019.

716 Nieberding F., Wille C., Ma Y., Wang Y., Maurischat P., Lehnert L. et al.: Winter daytime warming and
717 shift in summer monsoon increase plant cover and net CO₂ uptake in a central Tibetan alpine
718 steppe ecosystem. *J. Geophys. Res. Biogeosci.*, 2021.

719 Sankar M.S., Dash P., Lu Y. et al.: Land use and land cover control on the spatial variation of dissolved
720 organic matter across 41 lakes in Mississippi, USA. *Hydrobiol.*, 847, 1159–1176, 2020.

721 Oksanen J., Blanchet F.G., Friendly M., Kindt R., Legendre P., McGlinn D. et al.: *vegan: Community
722 Ecology Package*, 2020.

723 Osterholz H., Turner S., Alakangas L.J., Tullborg E.-L., Dittmar T., Kalinowski B.E. et al.: Terrigenous
724 dissolved organic matter persists in the energy-limited deep groundwaters of the Fennoscandian
725 Shield. *Nat Commun*, 13, 1, 4837, 2022.

726 Pohlabein A.M., Gomez-Saez G.V., Noriega-Ortega B.E., Dittmar T.: Experimental Evidence for Abiotic
727 Sulfurization of Marine Dissolved Organic Matter. *Frontiers in Marine Science*, 4,
728 <http://dx.doi.org/10.3389/fmars.2017.00364>, 2017.

729 Qiu, J.: China: The third pole. *Nature* 454, 2008.

730 Qu B., Zhang Y., Kang S., Sillanpää M.: Water quality in the Tibetan Plateau: Major ions and trace
731 elements in rivers of the “Water Tower of Asia”. *The Science of the total environment*, 649, 571–
732 81, 2019.

733 R Core Team. R: A language and environment for statistical computing. Vienna, Austria: R Foundation
734 for Statistical Computing, 2013.

735 Riedel T., Dittmar T.: A method detection limit for the analysis of natural organic matter via Fourier
736 transform ion cyclotron resonance mass spectrometry. *Anal. Chem.*, 86, 16, 2014.

737 Roebuck J.A., Seidel M., Dittmar T., Jaffé R.: Land Use Controls on the Spatial Variability of Dissolved
738 Black Carbon in a Subtropical Watershed. *Environmental science & technology*, 52, 15, 2018.

739 Roebuck J.A., Seidel M., Dittmar T., Jaffé R.: Controls of Land Use and the River Continuum Concept
740 on Dissolved Organic Matter Composition in an Anthropogenically Disturbed Subtropical
741 Watershed. *Environmental science & technology*, 54, 1, 2020.

742 Ruediger S.: Siberian River Run-Off in the Kara Sea: Characterisation, Quantification, Variability and
743 Environmental Significance, Elsevier, 2003.

744 Šantl-Temkiv T., Finster K., Dittmar T., Hansen B.M., Thyraug R., Nielsen N.W. et al.: Hailstones: a
745 window into the microbial and chemical inventory of a storm cloud. *PLOS ONE*, 8, 1, 2013.

746 Seidel M., Manecki M., Herlemann D.P.R., Deutsch B., Schulz-Bull D., Jürgens K. et al.: Composition
747 and Transformation of Dissolved Organic Matter in the Baltic Sea. *Front. Earth Sci.*, 5, G01004,
748 2017.

749 Seidel M., Yager P.L., Ward N.D., Carpenter E.J., Gomes H.R., Krusche A.V. et al.: Molecular-level
750 changes of dissolved organic matter along the Amazon River-to-ocean continuum. *Marine
751 Chemistry*, 177, 2015.

752 Seifert A.-G., Roth V.-N., Dittmar T., Gleixner G., Breuer L., Houska T., et al.: Comparing molecular
753 composition of dissolved organic matter in soil and stream water: Influence of land use and
754 chemical characteristics. *The Science of the total environment*, 571, 2016.

755 Singer G.A., Fasching C., Wilhelm L., Niggemann J., Steier P., Dittmar T. et al.: Biogeochemically
756 diverse organic matter in Alpine glaciers and its downstream fate. *Nature Geosci*, 5, 10, 2012.

757 Spencer R.G.M., Guo W., Raymond P.A., Dittmar T., Hood E., Fellman J. et al.: Source and biolability
758 of ancient dissolved organic matter in glacier and lake ecosystems on the Tibetan Plateau.
759 *Geochimica et Cosmochimica Acta*, 142, 2014.

760 Spencer R.G.M., Stubbins A., Hernes P.J., Baker A., Mopper K., Aufdenkampe A.K. et al.:
761 Photochemical degradation of dissolved organic matter and dissolved lignin phenols from the
762 Congo River. *J. Geophys. Res.*, 114, G3, 2009.

763 Telling J., Anesio A.M., Tranter M., Irvine-Fynn T., Hodson A., Butler C. et al.: Nitrogen fixation on
764 Arctic glaciers, Svalbard. *J. Geophys. Res.*, 116, G3, 2011.

765 Thukral A.K.. A review on measurement of Alpha diversity in biology. *Intern. Jour. Contemp.
766 Microbiol.*, 54, 1, 1, 2017.

767 Tran T.V., Buckel J., Maurischat P., Tang H., Yu Z., Hördt A. et al.: Delineation of a Quaternary Aquifer
768 Using Integrated Hydrogeological and Geophysical Estimation of Hydraulic Conductivity on the
769 Tibetan Plateau, China. *Water*, 13, 10, 2021.

770 van Dongen B.E., Zencak Z., Gustafsson Ö.: Differential transport and degradation of bulk organic
771 carbon and specific terrestrial biomarkers in the surface waters of a sub-arctic brackish bay
772 mixing zone. *Marine Chemistry*, 112, 3-4, 2008.

773 Vähätalo A.V., Wetzel R.G.: Photochemical and microbial decomposition of chromophoric dissolved
774 organic matter during long (months–years) exposures. *Mar. Chem.*, Vol. 89, 1–4, 313-326, 2004.

775 Wang H., Zhou X., Wan C., Fu H., Zhang F., Ren J.: Eco-environmental degradation in the northeastern
776 margin of the Qinghai–Tibetan Plateau and comprehensive ecological protection planning.
777 *Environ. Geol.* 55, 1135–1147, 2008.

778 Wang J., Huang L., Ju J., Daut G., Ma Q., Zhu L. et al.: Seasonal stratification of a deep, high-altitude,
779 dimictic lake: Nam Co, Tibetan Plateau. *Journal of Hydrology*, 584, 7, 2020.

780 Wang J., Zhu L., Daut G., Ju J., Lin X., Wang Y. et al.: Investigation of bathymetry and water quality of
781 Lake Nam Co, the largest lake on the central Tibetan Plateau, China. *Limnology*, 10, 2, 149–58,
782 2009.

783 Wang L., Zhang L., Cai W-J., Wang B., Yu Z.: Consumption of atmospheric CO₂ via chemical
784 weathering in the Yellow River basin: The Qinghai–Tibet Plateau is the main contributor to the
785 high dissolved inorganic carbon in the Yellow River. *Chemical Geology*, Vol. 430, 34-44, 2016.

786 Wickham H., Averick M., Bryan J., Chang W., McGowan L., François R. et al.: Welcome to the
787 Tidyverse. *JOSS*, 4, 43, 2019.

788 Wilson H.F., Xenopoulos M.A.: Effects of agricultural land use on the composition of fluvial dissolved
789 organic matter. *Nature Geosci*, 2, 1, <https://www.nature.com/articles/ngeo391>, 2009.

790 Wu X., Zhang W., Liu G., Yang X., Hu P., Chen T. et al.: Bacterial diversity in the foreland of the
791 Tianshan No. 1 glacier, China. *Ann. Glaciol.*, 7, 1, 14038, 2012.

792 Yao T.: Tackling on environmental changes in Tibetan Plateau with focus on water, ecosystem and
793 adaptation. *Sci. Bull. (Beijing)*. 64, 7, 417, 2019.

794 Yao T., Thompson L., Yang W. et al.: Different glacier status with atmospheric circulations in Tibetan
795 Plateau and surroundings. *Nature Clim. Change* 2, 2012.

796 Yoo H.-J., Choi Y.-J., Cho K.: Characterization of Natural Organic Matter in Spring Water. *Mass
797 Spectrometry Letters*, 11, 4, 2020.

798 Yu Z., Wu G., Li F., Chen M., Vi Tran T., Liu X. et al.: Glaciation enhanced chemical weathering in a cold
799 glacial catchment, western Nyangêntanglha Mountains, central Tibetan Plateau. *Journal of
800 Hydrology*, 597, 5, 2021.

801 Zhang Y., Wang G., Wang Y.: Changes in alpine wetland ecosystems of the Qinghai–Tibetan plateau
802 from 1967 to 2004. *Environ. Monit. Assess.* 180, 189–199, 2011.

803 Zhang Z., Qin J., Sun H., Yang J., Liu Y.: Spatiotemporal Dynamics of Dissolved Organic Carbon and
804 Freshwater Browning in the Zoige Alpine Wetland, Northeastern Qinghai-Tibetan Plateau. *Water*,
805 12, 9, 2020.

806